

Review



**Cite this article:** Le Roux A-L, Quiroga X, Walani N, Arroyo M, Roca-Cusachs P. 2019

The plasma membrane as a mechanochemical transducer. *Phil. Trans. R. Soc. B* **374**:

20180221.

<http://dx.doi.org/10.1098/rstb.2018.0221>

Accepted: 22 January 2019

One contribution of 13 to a discussion meeting issue 'Forces in cancer: interdisciplinary approaches in tumour mechanobiology'.

**Subject Areas:**

molecular biology, biomechanics, biophysics

**Keywords:**

plasma membrane, mechanotransduction, membrane tension, mechanosensor

**Authors for correspondence:**

Anabel-Lise Le Roux

e-mail: [aleroux@ibecbarcelona.eu](mailto:aleroux@ibecbarcelona.eu)

Pere Roca-Cusachs

e-mail: [proca@ibecbarcelona.eu](mailto:proca@ibecbarcelona.eu)

# The plasma membrane as a mechanochemical transducer

Anabel-Lise Le Roux<sup>1</sup>, Xarxa Quiroga<sup>1</sup>, Nikhil Walani<sup>2</sup>, Marino Arroyo<sup>1,2</sup> and Pere Roca-Cusachs<sup>1,3</sup>

<sup>1</sup>Institute for Bioengineering of Catalonia (IBEC), The Barcelona Institute for Science and Technology (BIST), Barcelona 08028, Spain

<sup>2</sup>LaCàN, Universitat Politècnica de Catalunya-BarcelonaTech, Spain

<sup>3</sup>Department of Biomedical Sciences, Universitat de Barcelona, Barcelona 08036, Spain

PR-C, 0000-0001-6947-961X

Cells are constantly submitted to external mechanical stresses, which they must withstand and respond to. By forming a physical boundary between cells and their environment that is also a biochemical platform, the plasma membrane (PM) is a key interface mediating both cellular response to mechanical stimuli, and subsequent biochemical responses. Here, we review the role of the PM as a mechanosensing structure. We first analyse how the PM responds to mechanical stresses, and then discuss how this mechanical response triggers downstream biochemical responses. The molecular players involved in PM mechanochemical transduction include sensors of membrane unfolding, membrane tension, membrane curvature or membrane domain rearrangement. These sensors trigger signalling cascades fundamental both in healthy scenarios and in diseases such as cancer, which cells harness to maintain integrity, keep or restore homeostasis and adapt to their external environment.

This article is part of a discussion meeting issue 'Forces in cancer: interdisciplinary approaches in tumour mechanobiology'.

## 1. Introduction

By forming a physical boundary permitting the segregation of specific chemical reactions, the self-association of amphiphilic lipid molecules played an important role in the origin of life. Accordingly, the plasma membrane (PM) of prokaryotes and eukaryotes constitutes a fundamental border between the cell and its environment, and tightly regulates the exchanges between the inside and outside of the cell. Its physical state and integrity are crucial for cell survival, and a major function of the PM is to preserve its integrity and enable changes in cell shape. These changes occur in response not only to cell processes such as division, migration or spreading, but also to the constant external mechanical forces present in physiological scenarios. Mechanical stimuli destabilize cellular homeostasis and are strongly associated with cancer [1,2], and cells need to respond to either maintain their integrity or trigger appropriate responses.

In this context, the PM constitutes a crucial interface, since mechanical forces will result in a change of its state. Accordingly, extensive work (which we cite here non-exhaustively) has addressed how membrane tension interplays with the actin cytoskeleton (CSK) to regulate cell shape [3–5], motility [6–9] and polarity [10,11]. Correspondingly, many reviews discuss the feedback between membrane mechanical properties, CSK organization and cell dynamics [12–19]. Whereas in this review we will not analyse this feedback in detail, we will address a related and equally important topic: how the PM can harness mechanically induced changes in its state to itself act as a mechanosensor. We will first detail the different types of external mechanical stimuli that can be applied to the PM, and its subsequent

mechanical response. Then, we will review how this PM response triggers specific molecular mechanosensing events, mediated by diverse mechanosensory molecules that share a common principle: they are sensitive to a mechanical state of the PM, or to a change of this state. Accordingly, they transduce the external mechanical input transmitted from the PM into a biochemical response. To decouple the effect of each particular signal, we will not consider inputs composed of multiple mechanical signals (such as those usually present in three-dimensional geometries). Therefore, we limit the review to two-dimensional *in vitro* systems and examine the acute response of mammalian cells to a single mechanical input.

## 2. Effect of external mechanical stimuli on the plasma membrane

The highly complex PM delimits the cell, and is in permanent contact with its surroundings. As such, it constitutes a crucial interface, since interactions with or alterations from the external environment will result in a change of its mechanical state. Whereas all living cells (eukaryotic or prokaryotic) receive a large diversity of mechanical inputs, here we will focus on the PM of animal cells. Examples of such cells in a mechanically active environment include alveolar epithelial cells in lungs, which cyclically stretch and relax, or skin cells, which also experience transient stretch, but without a cyclic rhythm. Cells in the intestinal track withstand transmural pressure, shear flow and cyclic strains [20], and smooth muscle cells in the bladder [21] or in ocular cells [22] are exposed to hydrostatic pressure. Vascular endothelial cells, circulating cells such as red blood cells, and cells from the immune system are exposed to shear flows [23,24]. Among a plethora of other cells, circulating cells (RBC)s passing in the kidney medullae [25], cells in the renal medullae [26] and cells exposed to the environment undergo important osmotic changes, which will stretch or compress cells. Topography is another external crucial mechanical cue, as many adherent cells must physically adapt to a topographically heterogeneous substrate such as the extracellular matrix (ECM) [27]. From a mechanical perspective, these stimuli can be grouped as tensile stresses (as applied by cell stretching and hypo-osmotic treatments), compressive stresses (as applied by cell compression and hyper-osmotic treatments) and shear stresses (as applied by shear flows acting on adherent cells) [28]. In this section, we will focus on experiments mainly applying only one of these stimuli, and we will not analyse their combined effects (as could occur for instance in cells flowing through narrow constrictions) [29]. As such, we will not consider three-dimensional geometries as they would lead to complex mechanical inputs.

### (a) Tensile stresses

Tensile stresses on the PM are commonly applied through hypotonic treatments [30–32], both to adhering and suspended cells (figure 1*a*(i)). Cells respond by swelling, thereby expanding their volume. Such osmotic treatments raise the issue of potential chemical responses triggered in parallel to the mechanical response [33,34]. Alternatively, cells adhered to flexible membranes can be stretched uniaxially or equibiaxially [31,35] (figure 1*a*(ii)), thereby regulating PM area more directly. In both types of experiment, there is an

increase in PM apparent tension, a measure containing the PM tension and the tension induced by adhesion to the underlying CSK, to which the PM is strongly attached (see further details in box 2). Indeed, application of 40–70% osmotic treatments increases apparent tension in neuron cells [32], fibroblasts [3] and human leukaemia cells (HL-60) [36], and application of a 40% uniaxial stretch increases apparent tension in human leukaemia cells [36]. In these assays, tension most likely increases both in the PM and in the underlying cytoskeletal actin cortex. The CSK is in fact thought to have mechano protective effects on the poorly extensible PM, which resists only a 3–5% area expansion before lysis, or rupture [8,28]. The CSK prevents tension-induced PM rupture by absorbing part of the applied stress [33,37]. Consistently, apparent PM tensions in unstressed cells range from 0.03 to 0.3 mN m<sup>-1</sup> [16,38], far from the estimated rupture tension of a bilayer, 3–10 mN m<sup>-1</sup> [8,13,38,39].

Upon stress application, however, cells have multiple ways of supplying lipids to the PM to buffer tension increases. First, highly abundant PM folds (see box 1) flatten upon tensile stress application [15,30,31] (figure 1*a*(iv)). Caveolae are an important type of such folds [40], exerting a PM mechanoprotective role directly [41] (rather than through caveolae endocytosis). Second, exocytosis contributes to PM area expansion [35,42–45] by adding lipids to the bilayer. Exocytosis occurs in response to PM tension increase [38] (figure 1*a*(v)). Interestingly, simple membrane mechanics could drive this process, as stretching a supported lipid bilayer leads to passive absorption of liposomes sitting on top of it [46]. Similarly, endocytosis arrest has been associated with increased PM tension, as observed for instance during osmotic swelling of rat basophilic leukaemia (RBL) cells [47]. Here again, tension may facilitate molecularly driven exocytosis [38,39].

Overall, the cell capacity to expand its area under tensile stress will thus depend not only on the nature and the magnitude of the stretch, but also on the PM lipid reserves in the form of folds and endomembranes [48]. For instance, the abundance of caveolae is cell-type-dependent, and they are highly abundant specifically in smooth muscle cells (highly exposed to stretch), and in endothelial cells (highly exposed to shear flows) [49]. Moreover, cells have very different resting tensions depending on their type [17,33] and state [3,48] and may even display heterogeneous apparent tension distribution within the PM upon application of local stimuli [50]. Such differences may explain why the cellular response to osmotic treatment is strongly cell-type-dependent: in a range of cell types, PM area expansion prevented tension increases upon hypotonic treatments of 50%, but not of 98% [43]. However, in mouse lung endothelial (MLEC) cells, a 50% hypotonic treatment did not lead to an increase in tension unless caveolar proteins were knocked down [40]. Additionally, the physiological relevance of large osmotic treatments in most physiological situations was questioned in a recent study [51], and for instance a value of 20% (measured to be insufficient to affect tension) was found to be closer to physiological values in endothelial cells. In any case, the magnitude of osmotic treatment or stretch needed to increase PM tension after cells have depleted their lipid reserves, and its relationship to the relevant physiology of each cell type, remain an open question.

At the molecular level, an increase in PM tension (and thereby membrane area) is predicted to decrease its thickness,

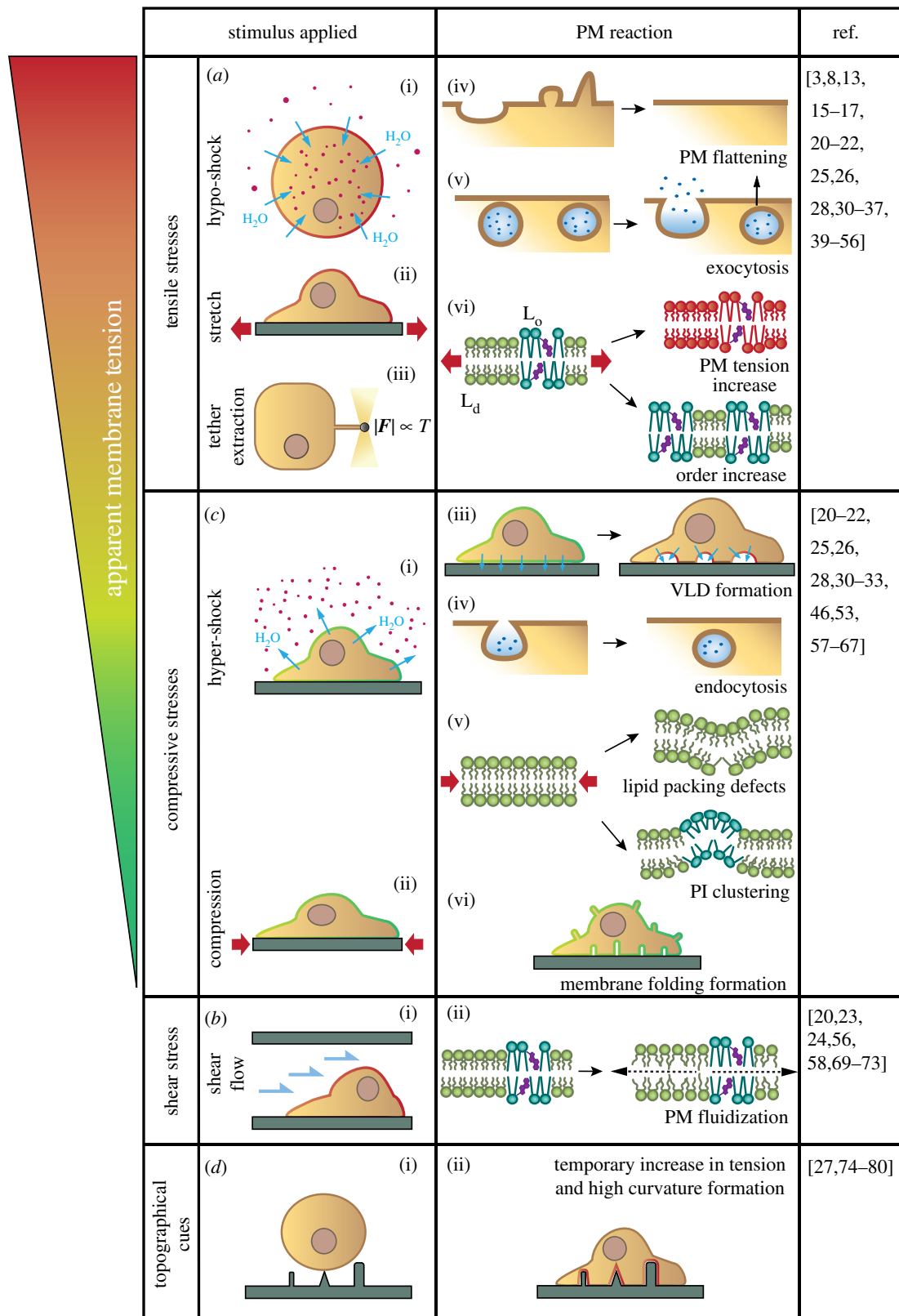


**Figure 1.** PM response to applied mechanical stimuli. (a) Tensile stresses are applied experimentally by tether pulling, hypotonic shocks and cell stretching. In response, PM folds flatten and exocytosis increases, buffering the increase in tension. Once lipid reserves have been used, PM tension and order increase. (b) Compressive stresses are applied experimentally through hyper-osmotic shocks and stretch release. In response, PM folds of different shapes and sizes form (vacuole-like dilations (VLDs), tubes), endocytosis increases, lipid packing defects appear in highly curved areas and phosphoinositide (PI) clusters form. (c) Shear stress application results in increased PM fluidity, in both  $L_o$  and  $L_d$  phases. (d) Upon encountering topographical cues, cells adapt their PM to substrate architecture, likely triggering a temporary increase in PM tension.

to minimize PM volume and the exposure of hydrophobic tails to water [28]. This could directly affect transmembrane protein conformation, decrease lipid packing and facilitate diffusion in the lipid bilayer. This was predicted in 1,2-

dioleoyl-*sn*-glycero-3-phosphocholine (DOPC) bilayers [52] and observed upon application of an osmotic treatment in synthetic giant unilamellar vesicles (GUVs) made of DOPC [53]. In GUVs of complex lipid composition, bilayer tension

**Box 1. Mechanical and molecular features of the plasma membrane**

The cellular PM has evolved to become an extremely complex entity, bearing an asymmetric bilayer considered as a two-dimensional fluid formed by glycerophospholipids, sphingolipids, cholesterol and carbohydrates, as well as high amounts of transmembrane or peripheral proteins. A key PM parameter is its fluidity (also referred as its reciprocal viscosity, which is the internal property of a fluid that offers resistance to flow [23]). Fluidity is commonly related to high molecular mobility in the bilayer, which enables lateral diffusion of the embedded molecules [73]. Diffusion in the PM is slower than in a pure lipid bilayer [179] because of its lateral organization, especially through the presence of peripheral and transmembrane proteins [180], its shape and its attachment to the cytoskeleton (CSK). The complex composition of the PM results in lateral liquid–liquid phase separation of the bilayer in liquid-disordered ( $L_d$ ) and liquid-ordered ( $L_o$ ) domains, with reduced diffusion in the latter.  $L_o$  domains in the PM (also called lipid rafts) are enriched in cholesterol, sphingolipids and transmembrane or anchored proteins, display a higher lipid packing and dynamically assemble and disassemble at a fast rate in domains of different sizes [181]. Of note, controversies remain about the organization and dynamics of these domains [182].

Another fundamental PM parameter is its topography. The PM has a spontaneous curvature conferred by its composition and asymmetry and is not a smooth bilayer [183]. It contains actively maintained folds in the form of micro- and nano-structures such as ruffles, microvilli or caveolae [13]. Among them, caveolae are small PM invaginations (20–100 nm) shaped by caveolin and cavin proteins [102,184,185]. Caveolae are enriched in glycosphingolipids and cholesterol but are apparently devoid of transmembrane proteins [186]. These folds are actively maintained through mechanochemical feedbacks which have been the object of many studies [80,132,187]. The PM is also strongly coupled to the CSK through different biochemical links. ERM proteins (ezrin, radixin and moesin proteins) [188] mediate PM attachment to the cortex, and actin filaments also attach to caveolae [184], lipid rafts [189] and recently described asters (actin-based PM nanoclusters) [181]. Such PM–CSK interaction may locally impair diffusion and organize the PM as a ‘fence and picket’ bilayer [190]. The PM constantly undergoes fusion (exocytic) and fission (endocytic) events through a variety of pathways [191], ensuring protein and lipid turnover as well as chemical communication with the outside environment. Endocytosis decreases PM area while exocytosis increases it.

triggered phase separation and appearance of liquid-ordered ( $L_o$ ) domains in the PM (see box 1) [53,54], which is in opposition to some theoretical predictions [55] (figure 1a(vi)). Increased PM order was also observed upon uniaxial stretch of vascular endothelial cells [56], coupled with a slower diffusion as assessed by FRAP (fluorescence recovery after photobleaching) measurement. Similarly, increased PM order occurred upon application of a hypoosmotic treatment in HeLa or MDCK cells [53]. Both effects (phase separation and lipid unpacking) would likely affect lipid raft organization and dynamics (see box 1). However, they would, respectively, increase or decrease packing and diffusion in the bilayer, and therefore the overall effect of PM tension remains unclear.

**(b) Compressive stresses**

When stretch is released, or if a hyperosmotic treatment is applied, a decrease in apparent tension has been consistently measured [32,57,58] (figure 1b(i,ii)). Compression also leads to PM bending [28]. In the case of hyperosmotic treatments (or restoration of medium tonicity after an isotonic treatment), dome-shaped micrometre-sized invaginations termed vacuole-like dilations (VLDs) form passively [31–33]. VLDs are only observed at the basal substrate-bound side of the PM (figure 1b(iii)), and we demonstrated that they were due to expulsion from cells of water which was not absorbed by hydrophobic substrates such as glass coverslips [31]. If cells are seeded on porous substrates, water can flow through and VLDs are not observed. Upon stretch release, passive PM folds also form, both in DOPC-supported lipid bilayers [46,59] and in the PM of several cell types [31] (figure 1b(vi)). These folds can be dot-shaped sub-micrometre structures termed reservoirs, or longer tubes, depending on the magnitude of de-stretch. Such structures locally deform

the PM, thereby accommodating the lipid excess caused by compression. Similarly, caveolae that had been unfolded by tensile stress re-form upon stress release [60]. Interestingly, VLDs can also form upon stretch release on poroelastic substrates, owing to water flow out of the substrate [31,61]. Thus, the PM can deform during compression, either by accommodating excess PM in small folds, or by generating VLDs to accommodate water effluxes. Unlike in the case of stretch, adaptation to osmotic changes does not seem to require the formation of PM structures to accommodate excess PM area, likely because, particularly in flat cells, changes in cell volume induced by osmotic treatments can be accommodated with very small changes in PM area. Consistently, another study reported that hypertonic treatments affected cell shape and volume but not PM topology [30]. In all cases and regardless of their nature, reservoirs, tubes and VLDs are subsequently actively re-absorbed in the PM after formation [31]. Endocytosis also intervenes as an additional mechanism for handling the extra lipids in the PM [62] (figure 1b(iv)).

Analogously to tensile stresses, compressive stresses also lead to lipid reorganization, owing to both decreased tension and formation of highly curved structures. Experiments in GUVs showed formation of lipid packing defects in highly curved structures [63,64] in both  $L_o$  and  $L_d$  phases [65], which may facilitate the insertion of hydrophobic molecules (figure 1b(v)). In addition, high bilayer curvature can lead to lipid sorting or changes in the lipid phases. Indeed, simulations revealed correlation between lipid clustering and lipid bilayer curvature [66]. Experimentally, pulling tubes from GUVs led to the enrichment of unsaturated compared with saturated lipids close to phase separation [67], short chain lipids have a preference for highly curved bilayers *in vitro* [63] and stretch release in yeast led to the formation of invaginations enriched in phosphoinositides (PIs) [58]

**Box 2. Plasma membrane tension**

The tension in a lipid bilayer membrane is defined as the force per unit length acting on a cross-section of a membrane [15,17,39]. Thus, PM tension is the in-plane tension, set by the nature of the lipids forming the bilayer and influenced by external forces acting on the PM of a cell. PM tension arises from hydrostatic or osmotic pressures from the cytosol, the forces exerted by the CSK and adhesion forces if the cells adheres to a substrate or other cells [15,17,39]. Whereas cell compression and micropipette aspiration can be used to assess cell tension [14], the most accurate technique involves pulling PM tethers (figure 1a(iii)) through atomic force microscopy, optical tweezers or magnetic tweezers [14,17], where tension is inferred from the resistance force exerted by the tether. As extensively explained [14,17,19], the tension measured with this set-up is an apparent tension containing the PM tension and the tension induced by adhesion to the underlying CSK, to which the PM is strongly attached. Tether experiments do not decouple them, except in measurements performed on PM areas detached from the CSK (blebs) [50]. Comparative measurements in or out of blebs have determined that the CSK often has a higher contribution to the apparent tension than the PM, pointing out the essential role of CSK–PM coupling [17]. Furthermore, because of the very slow equilibration of PM tension at cellular scales when coupled to the CSK, tether measurements in such a situation are a local reporter of a possibly heterogeneous tension distribution [50]. Thus, unravelling the effects of external mechanical stimuli on the PM, decoupled from those on the CSK, is an important challenge, which may be addressable through novel molecular fluorescence sensors of PM tension [53,69]. Interestingly, the cell CSK generates mechanical constraints on the PM similar to those arising from external physical forces, giving rise to comparable mechanochemical responses at the PM, with interesting implications in division, motility or spreading [3,8,14].

(figure 1b(v)). Finally, a decrease in the PM tension through hyperosmotic treatment has been associated with a decrease in  $L_o$  areas in HeLa cells [53], which would be expected to facilitate diffusion in the bilayer.

**(c) Shear stresses**

Different studies have consistently found a rapid increase in PM disorder upon shear flow application (figure 1c(i)), either by using Laurdan imaging (a membrane fluorescent dye sensitive to local membrane packing [56]), a molecular rotor probe [68] or an FRET-based molecular sensor [69] (figure 1c(ii)). Although shear flows exert both a tensile stress from the hydrostatic pressure and a shear stress on the PM [24,70], the effect was specifically attributed to shear stress in one of the studies [56]. In this study, the increased disorder was coupled to increased diffusion in both GUVs and cells. This fluidization occurs to both  $L_d$  and  $L_o$  domains (although at different time scales [71]), and in caveolae [72]. How shear stress leads to those effects is intriguing, but potential mechanisms include an increase in PM resistance to shear flow caused by  $L_o$  domains [73], or effects in membrane tension. Indeed, shear traction on the cell surface induced by shear flow may modify membrane tension and its uniformity, as reported in a recent study [69]. However, increased apparent tension has been associated with increased (rather than decreased) order, as discussed previously in this article.

**(d) Topographical cues**

The topography surrounding cells also constitutes a mechanical stimulus, in that the cellular PM that is at the interface will be forced to adapt to the shape of the substrate (figure 1d(i)). *In vivo*, cells are often in contact with the ECM, a very heterogeneous material presenting changes in topography that shape the PM [27]. To mimic rough or confined topographies, cells have been seeded on micropatterned substrates of a variety of shapes, confining cell adhesion to restricted areas [74–76]. As expected, cells

adapt their volume and area to the patterns. Nanoneedles [76], nanocones [77] or nanopillars [78] 50–500 nm in diameter have also been engineered on a substrate before cells were seeded on top. Electron microscopy images confirmed that the PM wrapped around the pillars, adopting a highly curved configuration [79] (figure 1d(ii)). Therefore, external topography deforms the PM, and probably also induces a temporary increase in tension [80].

**3. Plasma membrane mechanical state sensors**

When mechanical stimuli affect PM shape and tension, the cell responds to restore its homeostasis [33]. Fast responses occur to temporarily accommodate the new mechanical state of the PM and prevent cell lysis, while adaptive responses occur if the mechanical stimulus is repeated or maintained [81–83]. The signalling cascades triggered by the PM response rely on mechanotransduction events, in which specific mechanosensing molecules sense mechanically induced changes in the PM and trigger a biochemical response. Unravelling the nature and function of these molecules is highly relevant, since they are the first sensors in subsequent complex signalling cascades that define cell response. In this section, we will focus on the players relevant at short time scales, in response to the mechanical stimuli described above. Long-term cellular adaptation of cells to cyclic or permanent external mechanical stimuli (often abnormal and leading to disease states) goes beyond the scope of this review and we refer the reader to recent reviews on the topic [20,81].

**(a) Sensors of tensile and shear stresses****(i) Protein conformational changes: response to plasma membrane tension**

Mechanically gated channels (MGCs) are clear players in PM mechanotransduction [84–87]. MGCs are integral membrane proteins that undergo a conformational change in response to an area expansion of the PM (figure 2a). They are activated by

	sensors	molecular response	ref.
(a)	conformational change		
	MGCs opening		[15,22, 84–98]
(b)	protein relocation		
	shear stress		[56,70]
	caveolae flattening		[40,60, 100–102]
(c)	protein relocation		
	PLD2 release		[36,103]
(d)	protein relocation		
	BAR unbinding		[11,14, 105,106]
(a)	compressive stress and topography cues		
	curvature sensing		[63,78, 79, 108–124, 139,140]
(b)	compressive stress		
	domain formation and protein recruitment		[58,65]

**Figure 2.** Molecular sensors of PM mechanical state. (a) Mechanically induced conformational changes include MGC opening upon stretch (thereby enabling ion transport) and G protein dimerization under shear flow. (b) Mechanically induced protein relocation events. (top) With increased PM tension, caveolae flatten and its proteic components relocate by freely diffusing through the PM and/or the cytosol. These molecular players can subsequently activate different signalling pathways. (middle) PLD2 proteins are sequestered at PM invaginations. When they unfold, PLD2 is released and activates its partner mTORC2, which subsequently regulates actin network assembly. (bottom) BAR proteins respond to fold flattening by unbinding from the PM and diffusing into the cytoplasm. (c) Compressive stresses and topographical cues result in the formation of different types of PM curvature that can be recognized by BAR proteins through their positively charged BAR domain. Proteins containing ALPS motifs can also sense curvature by inserting their amphipathic helix in curved PM areas, where lipid packing defects are more abundant. (d) Clustering of PIs due to compressive stresses leads to TORC2 sequestering and inhibition of its activity.

an increase in tension due to PM stretch or suction (usually assessed through micropipette aspiration in electrophysiology assays), osmotic treatments and flow-induced shear stress [84,88,89]. In the case of shear stress, it is unclear whether the MGC responds to the shear stress itself, or to

the hydrostatic pressure stretching the cellular PM. The first, bacterial channels (large conductance mechanosensitive ion channel, MscL) to be discovered have been extensively studied. These channels are believed to undergo a conformational change triggered by increased PM tension and

related PM area expansion [90] ('force from lipid' concept [91,92]) but also possibly by the induced changes in PM thickness [93]. MscL channels are believed to open slightly before the PM reaches the rupture tension under area expansion [15,22], although this assumption may not be generalizable to the very different eukaryotic membranes. Eukaryotic PM channels include TRP (transient receptor potential) channels, potassium channels and Piezo channels [84,92,94], which have recently raised a lot of interest [95,95,96]. Their activation may be due generally to changes in PM tension, but also changes in curvature [87], and the tensions needed to activate them may not need to be as close to the rupture tension as previously believed [86,88,97]. Importantly, PM tensions include CSK contributions (see box 2), and therefore tensions needed to activate MGCs will be higher in PM regions attached to the CSK than in detached regions (blebs) or in proteo-liposomes lacking CSK [95,98]. Interestingly, whereas the important factor in PMs under stretch is generally considered to be bilayer expansion, changes in bilayer thickness may induce conformational changes by introducing a hydrophobic mismatch [28], and even clustering effects [99]. This may lead to a broader range of transmembrane proteins sensitive to PM tensile stress.

#### (ii) Protein conformational changes: response to fluidity

Shear stress in the PM has been linked to G protein activation, by triggering the required conformational change. Application of a shear flow resulting in increased PM fluidity seems to allow higher G protein rotational mobility, which facilitates the GDP to GTP exchange and subsequent activation [70] (figure 2*a*). Shear stress also induced phosphorylation of VEGFRs (vascular endothelial growth factor receptors) but the actual mechanism still needs to be unravelled [56].

#### (iii) Protein relocation: caveolae

Upon increased PM tension, caveolae disassemble and flatten, reducing and thereby buffering PM tension changes [40]. A primary consequence of caveolae flattening is to prevent an increase in PM tension upon stress. In terms of inducing downstream responses, PM tension buffering by caveolae could prevent MGC activation, exerting thus an indirect mechanotransduction role [100]. Beside this, caveolae disassembly facilitates the diffusion of some of their proteins (figure 2*b*). Indeed, upon application of hypo-osmotic treatment inducing a 20% swelling, an increase in non-caveolar CAV1 (caveolin-1) and a higher population of freely diffusing CAV1 have been measured in MLEC cells [40]. Subjecting myoblasts to a single fast stretch (20% uniaxial) released the binding of CAV3 (caveolin-3) to SRC (proto-oncogene tyrosine-protein kinase SRC), enhancing SRC activation [60]. In addition to caveolin release from caveolae to the bulk PM, cavin-1 (caveolae-associated protein 1) can also be released into the cytoplasm [40], and could subsequently interact with signalling effectors. Another protein, EHD2 (EH-domain-containing protein 2), has been recently shown to be released as a consequence of caveolae unfolding, and subsequently translocated to the nucleus [101]. Lipid trafficking also seems to be modified by caveolae disassembly. Interestingly, a decrease in sphingolipid packing was also measured upon caveolae flattening [60], resulting in an accelerated turnover of glycosphingolipid, which might insert more easily

into the unpacked flattened caveolae. Lastly, caveolae are actively refolded upon stretch release [40] (in an ATP- and actin-dependent manner) but this active mechanism has not been elucidated in detail. However, it may involve a sensing role of a BAR (Bin/amphiphysin/Rvs) protein domain (see discussion on BAR-domain proteins below), since PACSIN 2 (protein kinase C and casein kinase substrate in neurons protein 2), which contains a BAR domain, may participate in caveolae biogenesis [102]. PACSIN 2 could thereby be an initial sensor of bilayer tension decrease, as well as a linker to actin through its SH3 (Src homology 3) domain [102].

#### (iv) Protein relocation: unfolding of other invaginations

Upon mechanical stretch (micropipette aspiration of a PM patch at 5 kPa), a redistribution of Slm (phosphatidylinositol 4,5-bisphosphate-binding protein Slm) proteins between distinct PM domains has been observed in eisosomes (folded structures) from yeast [103]. This led to activation of TORC2 (target of rapamycin kinase complex 2) and sphingolipid metabolism regulation. A similar mechanism was described recently in neutrophils [36]. Application of a tensile stress (from either hypo-osmotic treatment or a 40% radial stretch) possibly unfolded PM invaginations leading to PLD2 (phospholipase D2) release (figure 2*b*), subsequently activating mTORC2 (mammalian TORC2) and limiting actin network assembly. Another example is that of the unfolding of PM ruffles, where MARCKS (myristoylated alanine-rich C-kinase substrate) proteins localize and supposedly capture PIs. Ruffle unfolding may relocate MARCKS proteins and consequently release PIs in the PM [104]. Finally, unbinding of BAR proteins (extensively discussed in the next section) may occur upon flattening of PM invaginations [11,14,105,106] (figure 2*b*). If accompanied by an increase in PM tension, theoretical predictions suggest that BAR protein oligomerization would become unfavourable [107]. All these phenomena may potentially be enhanced by phase separation associated with increased PM tension, leading to relocation of embedded or anchored proteins.

## 4. Sensors of compressive stress and topography

### (a) Curvature sensing: Bin/amphiphysin/Rvs proteins

PM deformations generated upon compression, or because of external topography, can lead to the formation of extremely curved structures that can be detected by curvature-sensing proteins (CSPs; figure 2*c*). Among them, BAR-domain proteins are particularly relevant. Unravelling the crystal structure of AMPH (amphiphysin) [108] as a domain forming a banana-shaped arrangement upon dimerization, the so-called N-BAR domain, shed light on the way how such domains would act as scaffolds on top of curved lipid bilayers. Thereafter, N-BAR domains have been described as having a high intrinsic curvature, capable of sensing and inducing PM curvature. The family of BAR-domain-bearing proteins expanded to include different intrinsic curvatures, notably when crystal structures of F-BAR (Fes/CIP4 homology-BAR) domains (with a shallower degree of curvature than N-BAR domains) [109], and subsequently I-BAR (inverse-BAR) domains [110] (with an inverted curvature relative to N-BAR domains) followed. These domains bind the acidic PM with the positive charges of the BAR domain facing the curved PM.

## (b) Curvature sensing: proteins with bilayer insertion motifs

In parallel, amphipathic helix motifs are another type of curvature-sensing domain (figure 2c). These helices might be structured in the soluble form of the protein, or be disordered domains folding upon interaction with the lipid bilayer. As has been discovered for ARFGAP1 (ADP-ribosylation factor GTPase-activating protein 1) [111], these helices screen lipid packing defects, where they can easily be buried. Curved areas of the bilayer generate more transient defects than planar regions, giving these helices curvature-sensing capabilities [112]. The helix of ARFGAP1 has given the name to a family of motifs, ALPS (amphipathic lipid packing sensors), but the mechanisms used by ALPS have since then been expanded to a wide range of amphipathic or hydrophobic motifs [113]. Alpha-synuclein and proteins with hydrophobic anchors (e.g. lipidated N-terminal domains) also sense lipid packing defects [114,115], and some reports suggest that many proteins containing such motifs have curvature-sensing properties [63,115]. However, there might be rules restricting curvature-sensing capabilities to some hydrophobic motifs with specific properties [112], or setting the sensed curvature size range [114]. N-BAR proteins also possess ALPS motifs, opening the debate about which motifs in the BAR superfamily of proteins are in fact sensing PM curvature [116]. Several studies found that ALPS motifs, rather than the BAR domains [117], were responsible for curvature sensing in AMPH and some F- and I-BAR proteins [118–120]. Some studies therefore claim that the sensing motif could be the ALPS motif only, with the driving force for its interaction with the PM being the density of defects rather than affinity [120]. How F-BARs or I-BARs that do not contain ALPS motifs would sense curvature is unclear, but crowding effects [121] or effects from the surrounding protein backbone [122] or the large disordered domains found in many of these proteins [123,124] could be involved. Most probably, the curvature sensing event is a cooperative process to which each of these domains contributes [125].

## (c) Sensing versus inducing curvature

If present at sufficiently high concentrations (as is often the case in assays *in vitro* or in overexpression conditions), CSPs not only sense, but also induce curvature [112,116,126]. Whether sensing and inducing are always mediated by the same physical mechanisms remains unclear, but theoretical models [80] suggest that curvature sensing and generation are two manifestations of a fundamental coupling between the bilayer free energy, the chemical potential of proteins and curvature. According to this view, sensing and generation would occur concomitantly in general and can only be uncoupled in situations such as dilute or highly crowded protein coverage or fixed membrane shape. Supporting this suggestion, AMPH has been shown to sense and generate curvature [126]. Accordingly, the curvature-inducing effect, analysed mainly via vesicle tubulation assays of GUVs *in vitro* [108], is often considered as proof that the proteins are also sensors [80]. In cells, CSPs organize and remodel the PM [127], and most studies focus on how these proteins actively induce curvature to optimize cellular functions such as endocytosis [128]. To decouple inducing from sensing effects, *in vitro* assays have been developed to study the sensing mechanisms only. These

include assays to analyse the sensing of tense liposomes of different curvatures [119,120], lipid tether assays [126,129] and techniques such as the use of wavy lipid bilayers [130] or membrane-tubes extruded from a supported lipid bilayer [131]. It is also important to note that it is more challenging to study convex than concave curved proteins, although the former can be achieved by using lipid tethers [132]. Additionally, though many simulations have been developed to describe CSP bilayer shaping mechanisms [132,133], some also specifically describe sensing mechanisms [134].

In cells, CSPs may also trigger transduction to a biochemical signalling cascade. CSPs usually possess additional domains that recruit other partners, and convey a biochemical signal in the cell. BAR proteins localize to curved spots in the cellular PM [108], but this does not enable us to distinguish whether they sense curved PM domains or if they are recruited by another means (via lipid binding for example) and subsequently shape the PM, especially when overexpression of BAR proteins (known to induce PM tubule formation [127]) is used. The capacity of curved PM areas to recruit BAR proteins and induce mechanotransduction has mostly been found in cellular processes where PM curvature is pre-existing, and not generated in response to external forces. For instance, in CME (clathrin-mediated endocytosis), the endocytic bud (generated by CSPs themselves) possibly recruits other CSP participating in the endocytic event [135], although it is not clear when and whether curvature or other signals recruit these proteins [136]. During filipodia formation and retraction, invaginations created by PM tension release recruit the F-BAR protein FBP17 (formin-binding protein 17) [11]. Similarly, ArhGAP44 (Rho GTPase-activating protein 44), an N-BAR protein, colocalizes to nanoscale deformations in neurons, inhibiting filipodia formation/exploration [137]. The N-BAR protein PICK1 (protein interacting with C kinase-1) is recruited to nanovesicles (insulin-containing granules) because of their high curvature [138]. Other than BAR proteins, ARFGAP1, which contains an ALPS motif, is recruited to PM deformations induced by coat protein complex COPI [111].

## (d) Curvature sensing of deformations induced by extracellular forces

Other than responding to pre-existing PM curved areas, an exciting possibility is that curvature sensing is also important in the context of PM reshaping by extracellular stresses. For instance, CSPs recruit to mechanically induced curved structures in bacteria [139], and to nanocone-shaped PM invaginations created by substrate topography [78,79]. In the study by Zhao *et al.* [78], engineering substrate topography through nanopillars of different sizes and shapes led to recruitment of CSPs of different types, from N-BAR to I-BAR. Additionally, topography-induced CSP recruitment triggered mechanotransduction by enhancing endocytosis, via the recruitment of endocytic proteins such as clathrin and DNM2 (dynamin-2). Inspired by this method, a later study [140] used fluorescent N-BAR overexpression at low concentration to detect locations of cellular PM invaginations.

As suggested by these works, endocytosis seems to be a major cell response downstream of PM mechanosensing. Recently, the CLIC-GEEC (clathrin-independent carrier and



GPI-AP enriched endosomal compartment) endocytic pathway has been demonstrated to respond to mechanical tension [62]. The pathway found is governed by VCL (vinculin) acting upstream of GBF1 (Golgi-specific brefeldin A-resistance guanine nucleotide exchange factor 1), but the actual molecular sensor of the change in tension remains unknown. Two BAR proteins involved in CLIC-GEEC endocytosis and acting downstream of GBF1/ARF1 (ADP-ribosylation factor 1), namely IRSP53 (insulin receptor substrate protein, also known as BAIAP2) and PICK1 [141], could potentially play a role. In different work, a burst in endocytosis mediated by the BAR protein GTPase regulator GRAF1 (also known as ARHGAP26, Rho GTPase-activating protein 26) was reported upon restoring medium tonicity after a harsh hypotonic treatment [105], but the driving factor of GRAF1 recruitment remained unclear. The treatment also led to formation of VLD and subsequent recruitment of GRAF1. However, whether the curvature of micrometre-sized VLDs matches the sensing capabilities of GRAF1 is unclear. Interestingly, endocytosis in both studies is mediated by accumulation of myristoylated ARF proteins. In those proteins and similarly to ALPS motifs, the myristoylated hydrophobic anchor could insert into the PM and sense curvature.

Unrelated to endocytosis, the F-BAR RhoGAP protein Spv1 (spermathecal physiology variant) also has an interesting mechanosensing role in egg fertilization in *Caenorhabditis elegans* [106]. In the relaxed spermatheca, Spv1 localizes to the apical PM, inhibiting Rho1/RhoA activity. The entry of oocytes into the spermatheca stretches spermatheca cells, probably unfolding and flattening Spv1-containing microvilli, and leading to Spv1 detachment from the PM. Rho1/RhoA activity is then promoted, inducing cell contraction and expulsion of the fertilized embryo to the uterus. In this study, it is not clear whether Spv1 is recruited to PM microvilli through curvature sensing or another mechanism, but it seems clear that tension increase and subsequent microvilli flattening lead to Spv1 detachment, triggering signalling [106]. Other than these examples, further curvature-sensing events and subsequent mechanochemical responses likely remain to be unravelled. For instance, the reservoirs we observed upon cellular destretch [31] might be regions for curvature-sensing-mediated mechanotransduction.

### (e) Sensing protein relocation: response to phase changes

Upon decreasing PM tension, PIs cluster in invaginated PM structures in yeast [58], possibly due to either lipid sorting or changes in lipid phases. PI clustering led to binding of the PH (pleckstrin homology) domain of TORC2 to the PI-enriched PM, and consequently drove TORC2 recruitment and inactivation (figure 2*d*). Further, the enrichment of lipid packing defects in curved  $L_0$  domains upon compression could affect the location of anchored proteins. For instance, N-RAS (GTPase NRas), which targets lipid packing defects, shows preference for  $L_d$  domains on flat bilayers, but for  $L_0$  domains in highly curved liposomes [65].

## 5. Theoretical modelling

Much of the current understanding of the PM as a mechanochemical transducer reviewed here is the result of close

interaction between experiments and theory. Theoretical models and simulations provide a framework to rationalize and predict both (1) how mechanical stimuli affect the PM, and (2) the complex ensuing PM mechanochemistry. Regarding (1), free-standing membranes are well described by classical Helfrich-like models, which consider the membrane as a continuum surface whose stable configurations minimize bending energy. This bending energy depends on the curvature of the surface, and is subject to constraints such as fixed volume or area (see also box 3). The mechanics of membranes adhered to deformable or active networks, however, is richer and far less explored. Continuum models have shown how the interaction between the PM and the actin CSK controls PM tension in pressurized blebbing cells [37], in motile cells [142] or during localized membrane perturbations [50]. These works highlight how friction or heterogeneous attachment to the CSK leads to significant tension gradients. Continuum simulations have also established the mechanisms by which membranes confined to deformable and possibly poroelastic substrates cope with excess area or interstitial fluid [59,61]. The PM-CSK interaction described by these continuum models ultimately depends on an intimate and dynamical coupling over multiple length scales [143,144], which remains to be fully understood. Turning to membrane mechanochemistry, phase separation in model membranes has been successfully modelled using molecular dynamics (MD) [145] and continuum thermodynamic models, which have also described the coupling between shape and composition [146,147]. The coupling between phase behaviour and tension, however, remains controversial since theoretical models predict mixing upon tension increase [55], whereas experiments suggest this and the opposite behaviour [54,148]. Furthermore, theoretical models having focused on model membranes; their applicability to the more heterogeneous and dynamical PM is unclear.

Much of membrane mechanochemistry hinges on the interaction between membranes and proteins [132]. To capture the specificity of these interactions, all-atom MD simulations have identified molecular mechanisms behind curvature generation [149] and maintenance [150] by BAR domains, or the gating of mechanosensitive channels by membrane tension [151]. At the expense of molecular specificity, coarse-grained MD simulations [152] have been able to reach micrometre-sized domains during microseconds to understand curvature sensing and generation by large numbers of isotropic [153] or banana-shaped proteins [154], and the tension-dependence of such processes [107].

These approaches are complementary to hybrid continuum/discrete models, which treat the membrane as a continuum elastic surface but treat individual proteins as discrete objects. Such hybrid models have examined how PM tension and elasticity control mechanosensitive channels [155], or protein-mediated interactions between curving proteins of different shapes [156,157]. They have also shown that the collective behaviour of many channels [158] or curving proteins [157,159] is fundamentally multibody, highlighting a fundamental gap between models for individual proteins and mean-field models treating proteins as concentrations [80]. The latter models couple Helfrich-like bending energies, in which the spontaneous curvature of the membrane depends on the concentration of curving proteins, with mean-field models for the free energy of the protein gas. Such mean-field models (such as that by Flory [160] and Huggins

**Box 3.** Box 3. Theoretical definitions.*(a) Continuum models*

Continuum models treat the PM as a continuous surface rather than resolving individual lipid molecules. This results in a mean field description of the response of the PM.

*(b) Continuum Helfrich model*

This model treats the PM as a surface whose local area cannot be easily changed (inextensibility), which can shear in-plane without storing elastic energy because it is fluid, and which stores elastic energy when it is bent. Mathematically, this leads to an energy function that penalizes deviations between the local curvature of the surface and a spontaneous curvature encoding the bilayer asymmetry. Helfrich conceived of such a model in 1973 [192].

*(c) Flory–Huggins model*

This model describes the free energy of mixtures of fluids or gases. One can imagine a simplest mixture to be binary. If the mixture consists of repelling fluid particles, a low-energy state can be devised in which particles will segregate into distinct pure phases. At finite temperature, however, the mixture will have a tendency to maximize entropy, which favours a homogeneous mixture. In general, these two mechanisms will compete. Since the entropic response depends on the temperature, one can envision a critical temperature for repelling fluid mixtures beyond which the mixture would be homogeneous, while the phases are separated for temperatures below the critical temperature. Such a model was conceived by Flory and Huggins in the 1940s [160,161] to describe the behaviour of a mixture of polymers and has hence been used to predict the response of various kinds of mixtures. When applied to protein gases on fluid membranes, curvature modifies the energy required to place a protein molecule in a given membrane location (its chemical potential), which can lead to protein-rich curved domains in conditions where a planar membrane would remain homogeneously mixed.

[161]) account for the mixing entropy of the proteins in the membrane, and the self-interaction between proteins (see also box 3). Such thermodynamic continuum models provide a self-consistent description of curvature sensing, sorting [126] and generation, as well as its coupling with membrane tension [162]. Strikingly, despite the fact that these phenomena can be highly dynamical and concomitant, current theories have focused on equilibrium, or considered restricted dynamics with either fixed shape [163] or fixed protein coverage [164]. Looking forward, a fundamental challenge in the field is to connect models capturing protein–lipid specificity and membrane mechanochemistry at a mesoscale.

## 6. Concluding remarks

Though external mechanical forces play a crucial role in cell fate, the role of mechanochemical feedback mediated by the cellular PM remains largely unexplored. To further advance in this promising area, several aspects need to be considered. First, PM homeostasis is highly cell-dependent, and efforts need to be made to mimic physiological forces as closely as possible. Second, the respective effects of the PM and the underlying CSK need to be further clarified, as both can be sensitive to similar stimuli and can modify each other. For instance, a protein recruited to focal adhesions, Vinculin, was recently described as an early player in the endocytosis response triggered by PM compression due to stretch release [62]. Relatedly, changes in the PM order induced by cell shape have been associated with CSK reorganization [75]. In this regard, recently described molecular probes of PM tension [53] are promising tools to distinguish between these effects. Third, the respective roles and mechanisms of curvature sensing and inducing need to be further clarified. If all proteins bearing a hydrophobic anchor can sense curvature, this implies a future important broadening of the field,

especially if a combined effect with phase transition occurs as with N-Ras recruitment to  $L_o$  domains in curved liposomes. Fourth, this review also highlights the interplay between tension and curvature sensing, and both seem to play a role in biochemical sensing mechanisms. In addition, external forces exerted on the PM trigger molecular rearrangements such as phase changes or lipid sorting, possibly affecting directly many signalling proteins [165]. Finally, many CSPs have been explored at the nanoscale, but how cells sense curvature at the microscale remains unclear [166]. Upon cellular compression, structures of very different sizes can be generated [31], and may induce very different curvature-sensing mechanisms. To conclude, mechanotransduction by the cellular PM is still an emerging field, which could even have implications in other cellular membranes [167], including the nuclear membrane [168,169]. Here, we explored the short-term mechanotransduction events involved. Interestingly, several of the molecular players discussed (BAR proteins [170–172], TORC2 [173], MGCs [174] Arf1 [175,176] and caveolae [177,178]) are involved in different cancer scenarios, potentially through altered mechanical responses. However, how this occurs, and how it is linked to long-term cellular response to mechanical signals, remains as an open question and is likely to be an exciting area of research.

**Data accessibility.** This article does not contain any additional data.

**Authors' contributions.** A.-L.L.R., M.A., N.W. and P.R.-C. conceived the work and drafted the text. X.Q. illustrated the figures, with inputs from A.-L.L.R. and P.R.-C.

**Competing interests.** We declare we have no competing interests.

**Funding.** This work was supported by the Spanish Ministry of Science and Innovation (DPI2015-71789-R to M.A. and BFU2016-79916-P to P.R.-C.), the European Commission (H2020-FETPROACT-01-2016-731957 to M.A. and P.R.-C.), the European Research Council (CoG-681434 to M.A.), the Generalitat de Catalunya (2017-SGR-1602 to P.R.-C.), the prize 'ICREA Academia' for excellence in research (to M.A. and P.R.-C.), and Obra Social 'La Caixa'.

1. Northey JJ, Przybyla L, Weaver VM. 2017 Tissue force programs cell fate and tumor aggression. *Cancer Discovery* **7**, 1224–1237. (doi:10.1158/2159-8290.CD-16-0733)
2. Faurobert E, Bouin A-P, Albiges-Rizo C. 2015 Microenvironment, tumor cell plasticity, and cancer. *Curr. Opin. Oncol.* **27**, 64–70. (doi:10.1097/CCO.000000000000154)
3. Pontes B *et al.* 2017 Membrane tension controls adhesion positioning at the leading edge of cells. *J. Cell Biol.* **216**, 2959. (doi:10.1083/jcb.201611117)
4. Chugh P *et al.* 2017 Actin cortex architecture regulates cell surface tension. *Nat. Cell Biol.* **19**, 689–697. (doi:10.1038/ncb3525)
5. Simon C, Caorsi V, Campillo C, Sykes C. 2018 Interplay between membrane tension and the actin cytoskeleton determines shape changes. *Phys. Biol.* **15**, 65004. (doi:10.1088/1478-3975/aad1ab)
6. Gauthier NC, Fardin MA, Roca-Cusachs P, Sheetz MP. 2011 Temporary increase in plasma membrane tension coordinates the activation of exocytosis and contraction during cell spreading. *Proc. Natl Acad. Sci. USA* **108**, 14 467–14 472. (doi:10.1073/pnas.1105845108)
7. Lieber AD, Schweitzer Y, Kozlov MM, Keren K. 2015 Front-to-rear membrane tension gradient in rapidly moving cells. *Biophys. J.* **108**, 1599–1603. (doi:10.1016/j.bpj.2015.02.007)
8. Lieber AD, Yehudai-Resheff S, Barnhart EL, Theriot JA, Keren K. 2013 Membrane tension in rapidly moving cells is determined by cytoskeletal forces. *Curr. Biol.* **23**, 1409–1417. (doi:10.1016/j.cub.2013.05.063)
9. Hetmanski JHR *et al.* 2018 Membrane tension orchestrates rear retraction in matrix directed cell migration. *Sneak Peak*. (doi:10.2139/ssrn.3249468)
10. Houk AR *et al.* 2012 Membrane tension maintains cell polarity by confining signals to the leading edge during neutrophil migration. *Cell* **148**, 175–188. (doi:10.1016/j.cell.2011.10.050)
11. Tsujita K, Takenawa T, Itoh T. 2015 Feedback regulation between plasma membrane tension and membrane-bending proteins organizes cell polarity during leading edge formation. *Nat. Cell Biol.* **17**, 749–758. (doi:10.1038/ncb3162)
12. Keren K. 2011 Cell motility: the integrating role of the plasma membrane. *Eur. Biophys. J.* **40**, 1013–1027. (doi:10.1007/s00249-011-0741-0)
13. Gauthier NC, Masters TA, Sheetz MP. 2012 Mechanical feedback between membrane tension and dynamics. *Trends Cell Biol.* **22**, 527–535. (doi:10.1016/j.tcb.2012.07.005)
14. Diz-Muñoz A, Fletcher DA, Weiner OD. 2013 Use the force: membrane tension as an organizer of cell shape and motility. *Trends Cell Biol.* **23**, 47–53. (doi:10.1016/j.tcb.2012.09.006)
15. Clark AG, Wartlick O, Salbreux G, Paluch EK. 2014 Stresses at the cell surface during animal cell morphogenesis. *Curr. Biol.* **24**, R484–R494. (doi:10.1016/j.cub.2014.03.059)
16. Sens P, Plastino J. 2015 Membrane tension and cytoskeleton organization in cell motility. *J. Phys. Condens. Matter* **27**, 273103. (doi:10.1088/0953-8984/27/27/273103)
17. Pontes B, Monzo P, Gauthier NC. 2017 Membrane tension: a challenging but universal physical parameter in cell biology. *Semin. Cell Dev. Biol.* **71**, 30–41. (doi:10.1016/j.semdb.2017.08.030)
18. Saha S, Nagy TL, Weiner OD. 2018 Joining forces: crosstalk between biochemical signalling and physical forces orchestrates cellular polarity and dynamics. *Phil. Trans. R. Soc. B* **373**, 20170145. (doi:10.1098/rstb.2017.0145)
19. Diz-Muñoz A, Weiner OD, Fletcher DA. 2018 In pursuit of the mechanics that shape cell surfaces. *Nat. Phys.* **14**, 648–652. (doi:10.1038/s41567-018-0187-8)
20. Gayer CP, Basson MD. 2009 The effects of mechanical forces on intestinal physiology and pathology. *Cell. Signal.* **21**, 1237–1244. (doi:10.1016/j.cellsig.2009.02.011)
21. Olsen SM, Stover JD, Nagatomi J. 2010 Examining the role of mechanosensitive ion channels in pressure mechanotransduction in rat bladder urothelial cells. *Ann. Biomed. Eng.* **39**, 688–697. (doi:10.1007/s10439-010-0203-3)
22. Kalapesi FB, Tan JC, Coroneo MT. 2005 Stretch-activated channels: a mini-review. Are stretch-activated channels an ocular barometer? *Clin. Exp. Ophthalmol.* **33**, 210–217. (doi:10.1111/j.1442-9071.2005.00981.x)
23. Theodoros G, Papaioannou CS. 2005 Vascular wall shear stress: basic principles and methods. *Hellen. J. Cardiol.* **46**, 9–15.
24. Wang Y, Dimitrakopoulos P. 2006 Nature of the hemodynamic forces exerted on vascular endothelial cells or leukocytes adhering to the surface of blood vessels. *Phys. Fluids* **18**, 87107. (doi:10.1063/1.2336116)
25. Lang F, Busch GL, Ritter M, Völkl H, Waldegger S, Gulbins E. 1998 Functional significance of cell volume regulatory mechanisms. *Physiol. Rev.* **78**, 247–306. (doi:10.1152/physrev.1998.78.1.247)
26. Kültz D. 2001 Cellular osmoregulation: beyond ion transport and cell volume. *Zoology* **104**, 198–208. (doi:10.1078/0944-2006-00025)
27. Kane R, Ma PX. 2013 Mimicking the nanostructure of bone matrix to regenerate bone. *Mater. Today* **16**, 418–423. (doi:10.1016/j.mattod.2013.11.001)
28. Hamill OP, Martinac B. 2001 Molecular basis of mechanotransduction in living cells. *Physiol. Rev.* **81**, 685–740. (doi:10.1152/physrev.2001.81.2.685)
29. Verstraeten SV, Mackenzie GG, Oteiza PI. 2010 The plasma membrane plays a central role in cells response to mechanical stress. *Biochim. Biophys. Acta Biomembr.* **1798**, 1739–1749. (doi:10.1016/j.bbamem.2010.06.010)
30. Pietuch A, Brückner BR, Janshoff A. 2013 Membrane tension homeostasis of epithelial cells through surface area regulation in response to osmotic stress. *Biochim. Biophys. Acta Mol. Cell Res.* **1833**, 712–722. (doi:10.1016/j.bbamcr.2012.11.006)
31. Kosmalka AJ *et al.* 2015 Physical principles of membrane remodelling during cell mechanoadaptation. *Nat. Commun.* **6**, 7292. (doi:10.1038/ncomms8292)
32. Dai J, Sheetz MP, Wan X, Morris CE. 1998 Membrane tension in swelling and shrinking molluscan neurons. *J. Neurosci.* **18**, 6681–6692. (doi:10.1523/jneurosci.18-17-06681.1998)
33. Morris CE, Homann U. 2001 Cell surface area regulation and membrane tension. *J. Membr. Biol.* **179**, 79–102. (doi:10.1007/s002320010040)
34. Jiang H, Sun SX. 2013 Cellular pressure and volume regulation and implications for cell mechanics. *Biophys. J.* **105**, 609–619. (doi:10.1016/j.bpj.2013.06.021)
35. Vlahakis NE, Schroeder MA, Pagano RE, Hubmayr RD. 2001 Deformation-induced lipid trafficking in alveolar epithelial cells. *Am. J. Physiol. Lung Cell. Mol. Physiol.* **280**, 938–946. (doi:10.1152/ajplung.2001.280.5.938)
36. Diz-Muñoz A, Thurley K, Chintamen S, Altschuler SJ, Wu LF, Fletcher DA, Weiner OD. 2016 Membrane tension acts through PLD2 and mTORC2 to limit actin network assembly during neutrophil migration. *PLoS Biol.* **14**, e1002474. (doi:10.1371/journal.pbio.1002474)
37. Alert R, Casademunt J, Brugués J, Sens P. 2015 Model for probing membrane-cortex adhesion by micropipette aspiration and fluctuation spectroscopy. *Biophys. J.* **108**, 1878–1886. (doi:10.1016/j.bpj.2015.02.027)
38. Wang G, Galli T. 2018 Reciprocal link between cell biomechanics and exocytosis. *Traffic* **19**, 741–749. (doi:10.1111/tra.12584)
39. Kozlov MM, Chernomordik LV. 2015 Membrane tension and membrane fusion. *Curr. Opin. Struct. Biol.* **33**, 61–67. (doi:10.1016/j.sbi.2015.07.010)
40. Sinha B *et al.* 2011 Cells respond to mechanical stress by rapid disassembly of caveolae. *Cell* **144**, 402–413. (doi:10.1016/j.cell.2010.12.031)
41. Cheng JPX *et al.* 2015 Caveolae protect endothelial cells from membrane rupture during increased cardiac output. *J. Cell Biol.* **211**, 53–61. (doi:10.1083/jcb.201504042)
42. Fisher JL, Levitan I, Margulies SS. 2004 Plasma membrane surface increases with tonic stretch of alveolar epithelial cells. *Am. J. Respir. Cell Mol. Biol.* **31**, 200–208. (doi:10.1165/rcmb.2003-02240C)
43. Groulx N, Boudreaux F, Orlov SN, Grygorczyk R. 2006 Membrane reserves and hypotonic cell swelling. *J. Membr. Biol.* **214**, 43–56. (doi:10.1007/s00232-006-0080-8)
44. van der Wijk T, Tomassen SFB, Houtsmuller AB, de Jonge HR, Tilly BC. 2003 Increased vesicle recycling

- in response to osmotic cell swelling. *J. Biol. Chem.* **278**, 40020–40025. (doi:10.1074/jbc.m307603200)
45. Vlahakis NE, Schroeder MA, Pagano RE, Hubmayr RD. 2002 Role of deformation-induced lipid trafficking in the prevention of plasma membrane stress failure. *Am. J. Respir. Crit. Care Med.* **166**, 1282–1289. (doi:10.1164/rccm.200203-2070C)
  46. Staykova M, Holmes DP, Read C, Stone HA. 2011 Mechanics of surface area regulation in cells examined with confined lipid membranes. *Proc. Natl Acad. Sci. USA* **108**, 9084–9088. (doi:10.1073/pnas.1102358108)
  47. Dai J, Ting-Beall HP, Sheetz MP. 1997 The secretion-coupled endocytosis correlates with membrane tension changes in RBL 2H3 cells. *J. Gen. Physiol.* **110**, 1–10. (doi:10.1085/jgp.110.1.1)
  48. Jumaa MAA, Dewitt S, Hallett MB. 2017 Topographical interrogation of the living cell surface reveals its role in rapid cell shape changes during phagocytosis and spreading. *Sci. Rep.* **7**, 9790. (doi:10.1038/s41598-017-09761-6)
  49. Parton RG, Simons K. 2007 The multiple faces of caveolae. *Nat. Rev. Mol. Cell Biol.* **8**, 185–194. (doi:10.1038/nrm2122)
  50. Shi Z, Graber ZT, Baumgart T, Stone HA, Cohen AE. 2018 Cell membranes resist flow. *Cell* **175**, 1769–1779. (doi:10.1016/j.cell.2018.09.054)
  51. Ayea MAA, LeMaster E, Teng T, Lee J, Levitan I. 2018 Hypotonic challenge of endothelial cells increases membrane stiffness with no effect on tether force. *Biophys. J.* **114**, 929–938. (doi:10.1016/j.bpj.2017.12.032)
  52. Reddy AS, Warshaviak DT, Chachisvilis M. 2012 Effect of membrane tension on the physical properties of DOPC lipid bilayer membrane. *Biochim. Biophys. Acta Biomembr.* **1818**, 2271–2281. (doi:10.1016/j.bbamem.2012.05.006)
  53. Colom A, Derivery E, Soleimanpour S, Tomba C, Molin MD, Sakai N, Matile S. 2018 A fluorescent membrane tension probe. *Nat. Chem.* **10**, 1118–1125. (doi:10.1038/s41557-018-0127-3)
  54. Hamada T, Kishimoto Y, Nagasaki T, Takagi M. 2011 Lateral phase separation in tense membranes. *Soft Matter* **7**, 9061. (doi:10.1039/c1sm05948c)
  55. Uline MJ, Schick M, Szelefer I. 2012 Phase behavior of lipid bilayers under tension. *Biophys. J.* **102**, 517–522. (doi:10.1016/j.bpj.2011.12.050)
  56. Yamamoto K, Ando J. 2015 Vascular endothelial cell membranes differentiate between stretch and shear stress through transitions in their lipid phases. *Am. J. Physiol. Heart Circul. Physiol.* **309**, H1178–H1185. (doi:10.1152/ajpheart.00241.2015)
  57. Xie K, Yang Y, Jiang H. 2018 Controlling cellular volume via mechanical and physical properties of substrate. *Biophys. J.* **114**, 675–687. (doi:10.1016/j.bpj.2017.11.3785)
  58. Riggi M *et al.* 2018 Decrease in plasma membrane tension triggers PtdIns4,5P2 phase separation to inactivate TORC2. *Nat. Cell Biol.* **20**, 1043–1051. (doi:10.1038/s41556-018-0150-z)
  59. Staykova M, Arroyo M, Rahimi M, Stone HA. 2013 Confined bilayers passively regulate shape and stress. *Phys. Rev. Lett.* **110**, 028101. (doi:10.1103/PhysRevLett.110.028101)
  60. Gervasio OL, Phillips WD, Cole L, Allen DG. 2011 Caveolae respond to cell stretch and contribute to stretch-induced signaling. *J. Cell Sci.* **124**, 3581–3590. (doi:10.1242/jcs.084376)
  61. Casares L *et al.* 2015 Hydraulic fracture during epithelial stretching. *Nat. Mater.* **14**, 343–351. (doi:10.1038/nmat4206)
  62. Thottacherry JJ *et al.* 2018 Mechanochemical feedback control of dynamin independent endocytosis modulates membrane tension in adherent cells. *Nat. Commun.* **9**, 4217. (doi:10.1038/s41467-018-06738-5)
  63. Hatzakis NS *et al.* 2009 How curved membranes recruit amphipathic helices and protein anchoring motifs. *Nat. Chem. Biol.* **5**, 835–841. (doi:10.1038/nchembio.213)
  64. Pinot M, Vanni S, Ambroggio E, Guet D, Goud B, Manneville J-B. 2018 *Feedback between membrane tension, lipid shape and curvature in the formation of packing defects.* Cold Spring Harbor, NY: Cold Spring Harbor Laboratory.
  65. Larsen JB *et al.* 2015 Membrane curvature enables N-Ras lipid anchor sorting to liquid-ordered membrane phases. *Nat. Chem. Biol.* **11**, 192–194. (doi:10.1038/nchembio.1733)
  66. Koldsø H, Shorthouse D, Hélie J, Sansom MSP. 2014 Lipid clustering correlates with membrane curvature as revealed by molecular simulations of complex lipid bilayers. *PLoS Comput. Biol.* **10**, e1003911. (doi:10.1371/journal.pcbi.1003911)
  67. Callan-Jones A, Sorre B, Bassereau P. 2011 Curvature-driven lipid sorting in biomembranes. *Cold Spring Harb. Perspect. Biol.* **3**, a004648. (doi:10.1101/cshperspect.a004648)
  68. Haidekker MA, L'Heureux N, Frangos JA. 2000 Fluid shear stress increases membrane fluidity in endothelial cells: a study with DCVJ fluorescence. *Am. J. Physiol. Heart Circul. Physiol.* **278**, H1401–H1406. (doi:10.1152/ajpheart.2000.278.4.H1401)
  69. Li W, Yu X, Xie F, Zhang B, Shao S, Geng C, Aziz AR, Liao X, Liu B. 2018 A membrane-bound biosensor visualizes shear stress-induced inhomogeneous alteration of cell membrane tension. *iScience* **7**, 180–190. (doi:10.1016/j.isci.2018.09.002)
  70. White CR, Frangos JA. 2007 The shear stress of it all: the cell membrane and mechanochemical transduction. *Phil. Trans. R. Soc. B* **362**, 1459–1467. (doi:10.1098/rstb.2007.2128)
  71. Tabouillot T, Muddana HS, Butler PJ. 2010 Endothelial cell membrane sensitivity to shear stress is lipid domain dependent. *Cell. Mol. Bioeng.* **4**, 169–181. (doi:10.1007/s12195-010-0136-9)
  72. Yamamoto K, Ando J. 2013 Endothelial cell and model membranes respond to shear stress by rapidly decreasing the order of their lipid phases. *J. Cell Sci.* **126**, 1227–1234. (doi:10.1242/jcs.119628)
  73. Espinosa G, Lopez-Montero I, Monroy F, Langevin D. 2011 Shear rheology of lipid monolayers and insights on membrane fluidity. *Proc. Natl Acad. Sci. USA* **108**, 6008–6013. (doi:10.1073/pnas.1018572108)
  74. Fernandez A, Bautista M, Stanciuskas R, Chung T, Pinaud F. 2017 Cell-shaping micropatterns for quantitative super-resolution microscopy imaging of membrane mechanosensing proteins. *ACS Appl. Mater. Interfaces* **9**, 27 575–27 586. (doi:10.1021/acsami.7b09743)
  75. von Erlach TC *et al.* 2018 Cell-geometry-dependent changes in plasma membrane order direct stem cell signalling and fate. *Nat. Mater.* **17**, 237–242. (doi:10.1038/s41563-017-0014-0)
  76. Chiappini C, Martinez JO, De Rosa E, Almeida CS, Tasciotti E, Stevens MM. 2015 Biodegradable nanoneedles for localized delivery of nanoparticles *in vivo*: exploring the biointerface. *ACS Nano* **9**, 5500–5509. (doi:10.1021/acsnano.5b01490)
  77. Galic M, Jeong S, Tsai F-C, Joubert L-M, Wu YI, Hahn KM, Cui Y, Meyer T. 2012 External push and internal pull forces recruit curvature-sensing N-BAR domain proteins to the plasma membrane. *Nat. Cell Biol.* **14**, 874–881. (doi:10.1038/ncb2533)
  78. Zhao W *et al.* 2017 Nanoscale manipulation of membrane curvature for probing endocytosis in live cells. *Nat. Nanotechnol.* **12**, 750–756. (doi:10.1038/nnano.2017.98)
  79. Lou H-Y, Zhao W, Zeng Y, Cui B. 2018 The role of membrane curvature in nanoscale topography-induced intracellular signaling. *Acc. Chem. Res.* **51**, 1046–1053. (doi:10.1021/acs.accounts.7b00594)
  80. Baumgart T, Capraro BR, Zhu C, Das SL. 2011 Thermodynamics and mechanics of membrane curvature generation and sensing by proteins and lipids. *Annu. Rev. Phys. Chem.* **62**, 483–506. (doi:10.1146/annurev.physchem.012809.103450)
  81. Jufri NF, Mohamedali A, Avolio A, Baker MS. 2015 Mechanical stretch: physiological and pathological implications for human vascular endothelial cells. *Vascular Cell* **7**, 8. (doi:10.1186/s13221-015-0033-z)
  82. Chai Q, Wang X-L, Zeldin DC, Lee H-C. 2013 Role of caveolae in shear stress-mediated endothelium-dependent dilation in coronary arteries. *Cardiovasc. Res.* **100**, 151–159. (doi:10.1093/cvr/cvt157)
  83. Gudipaty SA, Lindblom J, Loftus PD, Redd MJ, Edes K, Davey CF, Krishnegowda V, Rosenblatt J. 2017 Mechanical stretch triggers rapid epithelial cell division through Piezo1. *Nature* **543**, 118–121. (doi:10.1038/nature21407)
  84. Ranade SS, Syeda R, Patapoutian A. 2015 Mechanically activated ion channels. *Neuron* **87**, 1162–1179. (doi:10.1016/j.neuron.2015.08.032)
  85. Battle AR, Ridone P, Bavi N, Nakayama Y, Nikolaev YA, Martinac B. 2015 Lipid–protein interactions: lessons learned from stress. *Biochim. Biophys. Acta Biomembr.* **1848**, 1744–1756. (doi:10.1016/j.bbamem.2015.04.012)
  86. Sachs F. 2018 Mechanical transduction and the dark energy of biology. *Biophys. J.* **114**, 3–9. (doi:10.1016/j.bpj.2017.10.035)

87. Martinac B, Bavi N, Ridone P, Nikolaev YA, Martinac AD, Nakayama Y, Rohde PR, Bavi O. 2018 Tuning ion channel mechanosensitivity by asymmetry of the transbilayer pressure profile. *Biophys. Rev.* **10**, 1377–1384. (doi:10.1007/s12551-018-0450-3)
88. Lewis AH, Grandl J. 2015 Mechanical sensitivity of Piezo1 ion channels can be tuned by cellular membrane tension. *eLife* **4**, e12088. (doi:10.7554/eLife.12088)
89. Gerhold KA, Schwartz MA. 2016 Ion channels in endothelial responses to fluid shear stress. *Physiology* **31**, 359–369. (doi:10.1152/physiol.00007.2016)
90. Haswell ES, Phillips R, Rees DC. 2011 Mechanosensitive channels: what can they do and how do they do it? *Structure* **19**, 1356–1369. (doi:10.1016/j.str.2011.09.005)
91. Teng J, Loukin S, Anishkin A, Kung C. 2014 The force-from-lipid (FFL) principle of mechanosensitivity, at large and in elements. *Pflügers Archiv Eur. J. Physiol.* **467**, 27–37. (doi:10.1007/s00424-014-1530-2)
92. Markin VS, Sachs F. 2004 Thermodynamics of mechanosensitivity. *Phys. Biol.* **1**, 110–124. (doi:10.1088/1478-3967/1/2/007)
93. Guo YR, MacKinnon R. 2017 Structure-based membrane dome mechanism for Piezo mechanosensitivity. *eLife* **6**, e33660. (doi:10.7554/eLife.33660)
94. Cox CD, Bavi N, Martinac B. 2017 Origin of the force. *Curr. Top. Membr.* **79**, 59–96. (doi:10.1016/bs.ctm.2016.09.001)
95. Cox CD *et al.* 2016 Removal of the mechanoprotective influence of the cytoskeleton reveals PIEZO1 is gated by bilayer tension. *Nat. Commun.* **7**, 10366. (doi:10.1038/ncomms10366)
96. Zhao Q, Wu K, Geng J, Chi S, Wang Y, Zhi P, Zhang M, Xiao B. 2016 Ion permeation and mechanotransduction mechanisms of mechanosensitive Piezo channels. *Neuron* **89**, 1248–1263. (doi:10.1016/j.neuron.2016.01.046)
97. Chesler AT, Szczot M. 2018 Portraits of a pressure sensor. *eLife* **7**, e34396. (doi:10.7554/eLife.34396)
98. Charras GT, Williams BA, Sims SM, Horton MA. 2004 Estimating the sensitivity of mechanosensitive ion channels to membrane strain and tension. *Biophys. J.* **87**, 2870–2884. (doi:10.1529/biophysj.104.040436)
99. Guigas G, Weiss M. 2009 Effects of protein crowding on membrane systems. *Biochim. Biophys. Acta Biomembr.* **1858**, 2441–2450. (doi:10.1016/j.bbmem.2015.12.021)
100. Kozera L, White E, Calaghan S. 2016 Caveolae act as membrane reserves which limit mechanosensitive  $I_{Cl,swell}$  channel activation during swelling in the rat ventricular myocyte. *PLoS ONE* **4**, e8312. (doi:10.1371/journal.pone.0008312)
101. Torrino S *et al.* 2018 EHD2 is a mechanotransducer connecting caveolae dynamics with gene transcription. *J. Cell Biol.* **217**, 4092–4105. (doi:10.1083/jcb.201801122)
102. Parton RG, del Pozo MA. 2013 Caveolae as plasma membrane sensors, protectors and organizers. *Nat. Rev. Mol. Cell Biol.* **14**, 98–112. (doi:10.1038/nrm3512)
103. Berchtold D *et al.* 2012 Plasma membrane stress induces delocalization of Slm proteins and activation of TORC2 to promote sphingolipid synthesis. *Nat. Cell Biol.* **14**, 542–547. (doi:10.1038/ncb2480)
104. Sheetz MP, Sable JE, Döbereiner H-G. 2006 Continuous membrane-cytoskeleton adhesion requires continuous accommodation to lipid and cytoskeleton dynamics. *Annu. Rev. Biophys. Biomol. Struct.* **35**, 417–434. (doi:10.1146/annurev.biophys.35.040405.102017)
105. Vidal-Quadras M *et al.* 2017 Endocytic turnover of Rab8 controls cell polarization. *J. Cell Sci.* **130**, 1147–1157. (doi:10.1242/jcs.195420)
106. Tan PY, Zaidel-Bar R. 2015 Transient membrane localization of SPV-1 drives cyclical actomyosin contractions in the *C. elegans* spermatheca. *Curr. Biol.* **25**, 141–151. (doi:10.1016/j.cub.2014.11.033)
107. Simunovic M, Voth GA. 2015 Membrane tension controls the assembly of curvature-generating proteins. *Nat. Commun.* **6**, 7219. (doi:10.1038/ncomms8219)
108. Peter BJ. 2004 BAR domains as sensors of membrane curvature: the amphiphysin BAR structure. *Science* **303**, 495–499. (doi:10.1126/science.1092586)
109. Frost A, De Camilli P, Unger VM. 2007 F-BAR proteins join the BAR family fold. *Structure* **15**, 751–753. (doi:10.1016/j.str.2007.06.006)
110. Millard TH, Bompard G, Heung MY, Dafforn TR, Scott DJ, Machesky LM. 2005 Structural basis of filopodia formation induced by the IRSp53/MIM homology domain of human IRSp53. *EMBO J.* **24**, 240–250. (doi:10.1038/sj.emboj.7600535)
111. Bigay J, Casella J-F, Drin G, Mesmin B, Antony B. 2005 ArfGAP1 responds to membrane curvature through the folding of a lipid packing sensor motif. *EMBO J.* **24**, 2244–2253. (doi:10.1038/sj.emboj.7600714)
112. Antony B. 2011 Mechanisms of membrane curvature sensing. *Annu. Rev. Biochem.* **80**, 101–123. (doi:10.1146/annurev-biochem-052809-155121)
113. Drin G, Casella J-F, Gautier R, Boehmer T, Schwartz TU, Antony B. 2007 A general amphipathic  $\alpha$ -helical motif for sensing membrane curvature. *Nat. Struct. Mol. Biol.* **14**, 138–146. (doi:10.1038/nsmb1194)
114. Drin G, Antony B. 2009 Amphipathic helices and membrane curvature. *FEBS Lett.* **584**, 1840–1847. (doi:10.1016/j.febslet.2009.10.022)
115. Madsen KL, Bhatia VK, Gether U, Stamou D. 2010 BAR domains, amphipathic helices and membrane-anchored proteins use the same mechanism to sense membrane curvature. *FEBS Lett.* **584**, 1848–1855. (doi:10.1016/j.febslet.2010.01.053)
116. Isas JM, Ambrosio MR, Hegde PB, Langen J, Langen R. 2015 Tubulation by amphiphysin requires concentration-dependent switching from wedging to scaffolding. *Structure* **23**, 873–881. (doi:10.1016/j.str.2015.02.014)
117. McDonald NA, Vander Kooi CW, Ohi MD, Gould KL. 2015 Oligomerization but not membrane bending underlies the function of certain F-BAR proteins in cell motility and cytokinesis. *Dev. Cell* **35**, 725–736. (doi:10.1016/j.devcel.2015.11.023)
118. Yamamoto H, Kondo A, Itoh T. 2018 A curvature-dependent membrane binding by tyrosine kinase Fer involves an intrinsically disordered region. *Biochem. Biophys. Res. Commun.* **495**, 1522–1527. (doi:10.1016/j.bbrc.2017.12.009)
119. Bhatia VK, Madsen KL, Bolinger P-Y, Kunding A, Hedegård P, Gether U, Stamou D. 2009 Amphipathic motifs in BAR domains are essential for membrane curvature sensing. *EMBO J.* **28**, 3303–3314. (doi:10.1038/emboj.2009.261)
120. Bhatia VK, Hatzakis NS, Stamou D. 2010 A unifying mechanism accounts for sensing of membrane curvature by BAR domains, amphipathic helices and membrane-anchored proteins. *Semin. Cell Dev. Biol.* **21**, 381–390. (doi:10.1016/j.semdb.2009.12.004)
121. Bradley RP, Radhakrishnan R. 2016 Curvature-undulation coupling as a basis for curvature sensing and generation in bilayer membranes. *Proc. Natl Acad. Sci. USA* **113**, E5117–E5124. (doi:10.1073/pnas.1605259113)
122. Doucet CM, Esmery N, de Saint-Jean M, Antony B. 2015 Membrane curvature sensing by amphipathic helices is modulated by the surrounding protein backbone. *PLoS ONE* **10**, e0137965. (doi:10.1371/journal.pone.0137965)
123. Busch DJ, Houser JR, Hayden CC, Sherman MB, Lafer EM, Stachowiak JC. 2015 Intrinsically disordered proteins drive membrane curvature. *Nat. Commun.* **6**, 7875. (doi:10.1038/ncomms8875)
124. Zeno WF, Baul U, Snead WT, DeGroot ACM, Wang L, Lafer EM, Thirumalai D, Stachowiak JC. 2018 Synergy between intrinsically disordered domains and structured proteins amplifies membrane curvature sensing. *Nat. Commun.* **91**, 10114–10118. (doi:10.1038/s41467-018-06532-3)
125. Chen Z, Zhu C, Kuo CJ, Robustelli J, Baumgart T. 2016 The N-terminal amphipathic helix of endophilin does not contribute to its molecular curvature generation capacity. *J. Am. Chem. Soc.* **138**, 14616–14622. (doi:10.1021/jacs.6b06820)
126. Sorre B, Callan-Jones A, Manzi J, Goud B, Prost J, Bassereau P, Roux A. 2011 Nature of curvature coupling of amphiphysin with membranes depends on its bound density. *Proc. Natl Acad. Sci. USA* **109**, 173–178. (doi:10.1073/pnas.1103594108)
127. Suetsugu S, Kurisu S, Takenawa T. 2014 Dynamic shaping of cellular membranes by phospholipids and membrane-deforming proteins. *Physiol. Rev.* **94**, 1219–1248. (doi:10.1152/physrev.00040.2013)
128. McMahon HT, Boucrot E. 2015 Membrane curvature at a glance. *J. Cell Sci.* **128**, 1065–1070. (doi:10.1242/jcs.114454)
129. Zhu C, Das SL, Baumgart T. 2012 Nonlinear sorting, curvature generation, and crowding of endophilin N-BAR on tubular membranes. *Biophys. J.* **102**, 1837–1845. (doi:10.1016/j.bpj.2012.03.039)

130. Hsieh W-T, Hsu C-J, Capraro BR, Wu T, Chen C-M, Yang S, Baumgart T. 2012 Curvature sorting of peripheral proteins on solid-supported wavy membranes. *Langmuir* **28**, 12 838–12 843. (doi:10.1021/la302205b)
131. Deo R, Kushwah MS, Kamerkar SC, Kadam NY, Dar S, Babu K, Srivastava A, Pucadyil TJ. 2018 ATP-dependent membrane remodeling links EHD1 functions to endocytic recycling. *Nat. Commun.* **9**, 5187. (doi:10.1038/s41467-018-07586-z)
132. Bassereau P *et al.* 2018 The 2018 biomembrane curvature and remodeling roadmap. *J. Phys. D Appl. Phys.* **51**, 343001. (doi:10.1088/1361-6463/aacb98)
133. Simunovic M *et al.* 2016 How curvature-generating proteins build scaffolds on membrane nanotubes. *Proc. Natl Acad. Sci. USA* **113**, 11 226–11 231. (doi:10.1073/pnas.1606943113)
134. Gómez-Llobregat J, Elías-Wolff F, Lindén M. 2016 Anisotropic membrane curvature sensing by amphipathic peptides. *Biophys. J.* **110**, 197–204. (doi:10.1016/j.bpj.2015.11.3512)
135. Kaksonen M, Roux A. 2018 Mechanisms of clathrin-mediated endocytosis. *Nat. Rev. Mol. Cell Biol.* **19**, 313–326. (doi:10.1038/nrm.2017.132)
136. Picco A, Kukulski W, Manenschijn HE, Specht T, Briggs JAG, Kaksonen M. 2018 The contributions of the actin machinery to endocytic membrane bending and vesicle formation. *Mol. Biol. Cell* **29**, 1346–1358. (doi:10.1091/mbc.E17-11-0688)
137. Galic M, Tsai F-C, Collins SR, Matis M, Bandara S, Meyer T. 2014 Dynamic recruitment of the curvature-sensitive protein ArhGAP44 to nanoscale membrane deformations limits exploratory filopodia initiation in neurons. *eLife* **3**, e03116. (doi:10.7554/eLife.03116)
138. Herlo R *et al.* 2018 An amphipathic helix directs cellular membrane curvature sensing and function of the BAR domain protein PICK1. *Cell Rep.* **23**, 2056–2069. (doi:10.1016/j.celrep.2018.04.074)
139. Ramamurthi KS, Lecuyer S, Stone HA, Losick R. 2009 Geometric cue for protein localization in a bacterium. *Science* **323**, 1354–1357. (doi:10.1126/science.1169218)
140. Goudarzi M *et al.* 2017 Bleb expansion in migrating cells depends on supply of membrane from cell surface invaginations. *Dev. Cell* **43**, 577–587. (doi:10.1016/j.devcel.2017.10.030)
141. Sathé M, Muthukrishnan G, Rae J, Disanza A, Thattai M, Scita G, Parton RG, Mayor S. 2018 Small GTPases and BAR domain proteins regulate branched actin polymerisation for clathrin and dynamin-independent endocytosis. *Nat. Commun.* **9**, 1835. (doi:10.1038/s41467-018-03955-w)
142. Fogelson B, Mogilner A. 2014 Computational estimates of membrane flow and tension gradient in motile cells. *PLoS ONE* **9**, e84524. (doi:10.1371/journal.pone.0084524)
143. Liu AP, Richmond DL, Maibaum L, Pronk S, Geissler PL, Fletcher DA. 2008 Membrane-induced bundling of actin filaments. *Nat. Phys.* **4**, 789–793. (doi:10.1038/nphys1071)
144. Weichsel J, Geissler PL. 2016 The more the tubular: dynamic bundling of actin filaments for membrane tube formation. *PLoS Comput. Biol.* **12**, e1004982. (doi:10.1371/journal.pcbi.1004982)
145. Bennett WFD, Tieleman DP. 2013 Computer simulations of lipid membrane domains. *Biochim. Biophys. Acta Biomembr.* **1828**, 1765–1776. (doi:10.1016/j.bbmem.2013.03.004)
146. Baumgart T, Das S, Webb WW, Jenkins JT. 2005 Membrane elasticity in giant vesicles with fluid phase coexistence. *Biophys. J.* **89**, 1067–1080. (doi:10.1529/biophysj.104.049692)
147. Ursell TS, Klug WS, Phillips R. 2009 Morphology and interaction between lipid domains. *Proc. Natl Acad. Sci. USA* **106**, 13 301–13 306. (doi:10.1073/pnas.0903825106)
148. Portet T, Gordon SE, Keller SL. 2012 Increasing membrane tension decreases miscibility temperatures; an experimental demonstration via micropipette aspiration. *Biophys. J.* **103**, 35–37. (doi:10.1016/j.bpj.2012.08.061)
149. Blood PD, Voth GA. 2006 Direct observation of Bin/amphiphysin/Rvs (BAR) domain-induced membrane curvature by means of molecular dynamics simulations. *Proc. Natl Acad. Sci. USA* **103**, 15 068–15 072. (doi:10.1073/pnas.0603917103)
150. Yu H, Schulten K. 2013 Membrane sculpting by F-BAR domains studied by molecular dynamics simulations. *PLoS Comput. Biol.* **9**, e1002892. (doi:10.1371/journal.pcbi.1002892)
151. Vanegas JM, Arroyo M. 2014 Force transduction and lipid binding in Mslc: a continuum-molecular approach. *PLoS ONE* **9**, e113947. (doi:10.1371/journal.pone.0113947)
152. Bradley R, Radhakrishnan R. 2013 Coarse-grained models for protein-cell membrane interactions. *Polymers* **5**, 890–936. (doi:10.3390/polym5030890)
153. Reynwar BJ, Illya G, Harmandaris VA, Müller MM, Kremer K, Deserno M. 2007 Aggregation and vesiculation of membrane proteins by curvature-mediated interactions. *Nature* **447**, 461–464. (doi:10.1038/nature05840)
154. Simunovic M, Mim C, Marlovits TC, Resch G, Unger VM, Voth GA. 2013 Protein-mediated transformation of lipid vesicles into tubular networks. *Biophys. J.* **105**, 711–719. (doi:10.1016/j.bpj.2013.06.039)
155. Wiggins P, Phillips R. 2005 Membrane-protein interactions in mechanosensitive channels. *Biophys. J.* **88**, 880–902. (doi:10.1529/biophysj.104.047431)
156. Reynwar BJ, Deserno M. 2011 Membrane-mediated interactions between circular particles in the strongly curved regime. *Soft Matter* **7**, 8567. (doi:10.1039/C1SM05358B)
157. Dommersnes PG, Fournier J-B. 2002 The many-body problem for anisotropic membrane inclusions and the self-assembly of ‘saddle’ defects into an ‘egg carton’. *Biophys. J.* **83**, 2898–2905. (doi:10.1016/S0006-3495(02)75299-5)
158. Kahraman O, Koch PD, Klug WS, Haselwandter CA. 2016 Bilayer-thickness-mediated interactions between integral membrane proteins. *Phys. Rev. E* **93**, 042410. (doi:10.1103/PhysRevE.93.042410)
159. Kim KS, Neu J, Oster G. 1998 Curvature-mediated interactions between membrane proteins. *Biophys. J.* **75**, 2274–2291. (doi:10.1016/S0006-3495(98)77672-6)
160. Flory PJ. 1942 Thermodynamics of high polymer solutions. *J. Chem. Phys.* **10**, 51–61. (doi:10.1063/1.1723621)
161. Huggins ML. 1941 Solutions of long chain compounds. *J. Chem. Phys.* **9**, 440. (doi:10.1063/1.1750930)
162. Shi Z, Baumgart T. 2015 Membrane tension and peripheral protein density mediate membrane shape transitions. *Nat. Commun.* **6**, 5974. (doi:10.1038/ncomms6974)
163. Katz S, Givli S. 2017 Curvature-induced spatial ordering of composition in lipid membranes. *Comput. Math. Methods Med.* **2017**, 7275131. (doi:10.1155/2017/7275131)
164. Kabaso D, Bobrovska N, Gózdź W, Gov N, Kralj-Iglič V, Veranič P. 2012 On the role of membrane anisotropy and BAR proteins in the stability of tubular membrane structures. *J. Biomech.* **45**, 231–238. (doi:10.1016/j.jbiomech.2011.10.039)
165. Daste F *et al.* 2017 Control of actin polymerization via the coincidence of phosphoinositides and high membrane curvature. *J. Cell Biol.* **216**, 3745–3765. (doi:10.1083/jcb.201704061)
166. Cannon KS, Woods BL, Gladfelter AS. 2017 The unsolved problem of how cells sense micron-scale curvature. *Trends Biochem. Sci.* **42**, 961–976. (doi:10.1016/j.tibs.2017.10.001)
167. Beedle AE, Williams A, Relat-Goberna J, Garcia-Manyes S. 2015 Mechanobiology—chemical origin of membrane mechanical resistance and force-dependent signaling. *Curr. Opin Chem. Biol.* **29**, 87–93. (doi:10.1016/j.cbpa.2015.09.019)
168. Enyedi B, Niethammer P. 2016 A case for the nuclear membrane as a mechanotransducer. *Cell. Mol. Bioeng.* **9**, 247–251. (doi:10.1007/s12195-016-0430-2)
169. Aureille J, Belaadi N, Guilly C. 2017 Mechanotransduction via the nuclear envelope: a distant reflection of the cell surface. *Curr. Opin. Cell Biol.* **44**, 59–67. (doi:10.1016/j.celb.2016.10.003)
170. Liu S, Xiong X, Zhao X, Yang X, Wang H. 2015 F-BAR family proteins, emerging regulators for cell membrane dynamic changes—from structure to human diseases. *J. Hematol. Oncol.* **8**, 47. (doi:10.1186/s13045-015-0144-2)
171. Chen Y, Aardema J, Misra A, Corey SJ. 2012 BAR proteins in cancer and blood disorders. *Int. J. Biochem. Mol. Biol.* **3**, 198–208.
172. Sundborger AC, Hinshaw JE. 2015 Dynamin and BAR proteins—safeguards against cancer. *Crit. Rev. Oncogen.* **20**, 475–484. (doi:10.1615/CritRevOncog.v20.i5-6.160)
173. Kuo Y, Huang H, Cai T, Wang T. 2015 Target of rapamycin complex 2 regulates cell growth via Myc in *Drosophila*. *Sci. Rep.* **5**, 10339. (doi:10.1038/srep10339)
174. Leanza L, Managò A, Zoratti M, Gulbins E, Szabo I. 2016 Pharmacological targeting of ion channels for cancer therapy: in vivo evidences. *Biochim. Biophys. Acta Mol. Cell Res.* **1863**, 1385–1397. (doi:10.1016/j.bbamcr.2015.11.032)

175. Casalou C, Faustino A, Barral DC. 2016 Arf proteins in cancer cell migration. *Small GTPases* **7**, 270–282. (doi:10.1080/21541248.2016.1228792)
176. Boulay P-L, Schlienger S, Lewis-Saravalli S, Vitale N, Ferbeyre G, Claing A. 2011 ARF1 controls proliferation of breast cancer cells by regulating the retinoblastoma protein. *Oncogene* **30**, 3846–3861. (doi:10.1038/onc.2011.100)
177. Lamaze C, Torrinio S. 2015 Caveolae and cancer: a new mechanical perspective. *Biomed. J.* **38**, 367. (doi:10.4103/2319-4170.164229)
178. Martinez-Outschoorn UE, Sotgia F, Lisanti MP. 2015 Caveolae and signalling in cancer. *Nat. Rev. Cancer* **15**, 225–237. (doi:10.1038/nrc3915)
179. Murase K *et al.* 2004 Ultrafine membrane compartments for molecular diffusion as revealed by single molecule techniques. *Biophys. J.* **86**, 4075–4093. (doi:10.1529/biophysj.103.035717)
180. Campillo C *et al.* 2013 Unexpected membrane dynamics unveiled by membrane nanotube extrusion. *Biophys. J.* **104**, 1248–1256. (doi:10.1016/j.bpj.2013.01.051)
181. Sezgin E, Levental I, Mayor S, Eggeling C. 2017 The mystery of membrane organization: composition, regulation and roles of lipid rafts. *Nat. Rev. Mol. Cell Biol.* **18**, 361–374. (doi:10.1038/nrm.2017.16)
182. Kraft ML. 2013 Plasma membrane organization and function: moving past lipid rafts. *Mol. Biol. Cell* **24**, 2765–2768. (doi:10.1091/mbc.e13-03-0165)
183. Parmryd I, Önfelt B. 2013 Consequences of membrane topography. *FEBS J.* **280**, 2775–2784. (doi:10.1111/febs.12209)
184. Echarri A, Del Pozo MA. 2015 Caveolae—mechanosensitive membrane invaginations linked to actin filaments. *J. Cell Sci.* **128**, 2747–2758. (doi:10.1242/jcs.153940)
185. Nassoy P, Lamaze C. 2012 Stressing caveolae new role in cell mechanics. *Trends Cell Biol.* **22**, 381–389. (doi:10.1016/j.tcb.2012.04.007)
186. Shvets E, Bitsikas V, Howard G, Hansen CG, Nichols BJ. 2015 Dynamic caveolae exclude bulk membrane proteins and are required for sorting of excess glycosphingolipids. *Nat. Commun.* **6**, 6867. (doi:10.1038/ncomms7867)
187. Jarsch IK, Daste F, Gallop JL. 2016 Membrane curvature in cell biology: an integration of molecular mechanisms. *J. Cell Biol.* **214**, 375–387. (doi:10.1083/jcb.201604003)
188. McClatchey AI. 2014 ERM proteins at a glance. *J. Cell Sci.* **127**, 3199–3204. (doi:10.1242/jcs.098343)
189. Chichili GR, Rodgers W. 2009 Cytoskeleton—membrane interactions in membrane raft structure. *Cell. Mol. Life Sci.* **66**, 2319–2328. (doi:10.1007/s00018-009-0022-6)
190. Kusumi A, Suzuki KGN, Kasai RS, Ritchie K, Fujiwara TK. 2011 Hierarchical mesoscale domain organization of the plasma membrane. *Trends Biochem. Sci.* **36**, 604–615. (doi:10.1016/j.tibs.2011.08.001)
191. Stefan CJ *et al.* 2017 Membrane dynamics and organelle biogenesis—lipid pipelines and vesicular carriers. *BMC Biol.* **15**, 102. (doi:10.1186/s12915-017-0432-0)
192. Helfrich W. 1973 Elastic properties of lipid bilayers: theory and possible experiments. *Z. Naturf. C* **28**, 693–703. (doi:10.1515/znc-1973-11-1209)